SPANDIDOS PUBLICATIONS

Combination of high-resolution magic angle spinning proton magnetic resonance spectroscopy and microscale genomics to type brain tumor biopsies

A. ARIA TZIKA[1,2], LOUKAS ASTRAKAS[1,2], HAIHUI CAO[1,2], DIONYSSIOS MINTZOPOULOS[1,2], OVIDIU C. ANDRONESI[1,2], MICHAEL MINDRINOS[3], JIANGWEN ZHANG[4], LAURENCE G. RAHME[5], KONSTANTINOS D. BLEKAS[6], ARISTIDIS C. LIKAS[6], NIKOLAS P. GALATSANOS[6], RONA S. CARROLL[7] and PETER M. BLACK[7]

[1]NMR Surgical Laboratory, Department of Surgery, Harvard Medical School and Massachusetts General Hospital; [2]Athinoula A. Martinos Center of Biomedical Imaging, Department of Radiology, Massachusetts General Hospital, Boston, MA 02114; [3]Department of Biochemistry, Stanford University School of Medicine, Stanford, CA 94305; [4]Bauer Center for Genomics Research, Harvard University, Cambridge, MA 02138; [5]Laboratory of Molecular Surgery, Department of Surgery, Harvard Medical School and Massachusetts General Hospital, Boston, MA 02114, USA; [6]Department of Computer Science, University of Ioannina, Ioannina 45110, Greece; [7]Department of Neurosurgery Brigham and Women's Hospital, Harvard Medical School, Boston, MA 02115, USA

Received April 2, 2007; Accepted May 4, 2007

Abstract. Advancements in the diagnosis and prognosis of brain tumor patients, and thus in their survival and quality of life, can be achieved using biomarkers that facilitate improved tumor typing. We introduce and implement a combinatorial metabolic and molecular approach that applies state-of-the-art, high-resolution magic angle spinning (HRMAS) proton (^{1}H) MRS and gene transcriptome profiling to intact brain tumor biopsies, to identify unique biomarker profiles of brain tumors. Our results show that samples as small as 2 mg can be successfully processed, the HRMAS ^{1}H MRS procedure does not result in mRNA degradation, and minute mRNA amounts yield high-quality genomic data. The MRS and genomic analyses demonstrate that CNS tumors have altered levels of specific ^{1}H MRS metabolites that directly correspond to altered expression of Kennedy pathway genes; and exhibit rapid phospholipid turnover, which coincides with upregulation of cell proliferation genes. The data also suggest Sonic Hedgehog pathway (SHH) dysregulation may play a role in anaplastic ganglioglioma pathogenesis. That a strong correlation is seen between the HRMAS ^{1}H MRS and genomic data cross-validates and further demonstrates the biological relevance of the MRS results. Our combined metabolic/molecular MRS/genomic approach provides insights into the biology of anaplastic ganglioglioma and a new potential tumor typing methodology that could aid neurologists and neurosurgeons to improve the diagnosis, treatment, and ongoing evaluation of brain tumor patients.

Correspondence to: Dr A. Aria Tzika, NMR Surgical Laboratory, Department of Surgery, Massachusetts General Hospital and Harvard Medical School, 51 Blossom Street, Room 261, Boston, MA 02114, USA
E-mail: atzika@hms.harvard.edu

Key words: brain/CNS cancers, tumor biomarkers, anaplastic ganglioglioma, *ex vivo* high-resolution magic angle spinning magnetic resonance spectroscopy, genomics

Introduction

Magnetic resonance spectroscopic (MRS) studies of brain biomarkers can provide statistically significant biomarkers for tumor grade differentiation and improved predictors of cancer patient survival (1). *Ex vivo* high-resolution magic angle spinning (HRMAS) proton (^{1}H) MRS of unprocessed tissue samples (2) can help interpret *in vivo* ^{1}H MRS results, to improve the analysis of micro-heterogeneity in high-grade tumors (3); and provide insights into the relationships between clinically relevant cell processes and specific metabolites, such as choline-containing compounds involved in phospholipid metabolism, and lipids involved in apoptosis leading to necrosis (4). Furthermore, two-dimensional HRMAS ^{1}H MRS enables more detailed and unequivocal assignments of biologically important metabolites in intact tissue samples (5). Concurrently, a major focus in cancer research is to identify genes, using DNA-microarrays, that are aberrantly expressed in tumor cells, and to use their aberrant expression as biomarkers that correspond to and facilitate precise diagnoses and/or therapy outcomes of malignant transformation (6,7). Furthermore, comprehensive understanding of gene expression changes in specific tumor types should also greatly aid tumor analysis and the development of new treatment regimens.

While several studies have utilized MRS data or genomic data to promote cancer classification, to date these two methods

have not been combined and cross-validated to analyze the same cancer samples. Herein, we implement a combined quantitative biochemical and molecular approach to identify diagnostic biomarker profiles for CNS tumor fingerprinting that can facilitate the efficient monitoring of anticancer therapies and improve the survival and quality of life of cancer patients. We applied MRS and transcriptome profiling analyses to control and brain tumor biopsies, and to biopsies of anaplastic gangliogliomas, which are unusual CNS tumors of unknown biological behavior comprised of ganglion and glia cells that have cytologic features of neoplasia and are classified by WHO as distinct subsets (8). Significantly, the MRS and genomic data strongly correlate, to further demonstrate the biological relevance of MRS for tumor typing. Also, the levels of specific metabolites, such as choline containing metabolites, are altered in tumor tissue, and these changes correspond to the differential expression of Kennedy cycle genes responsible for the biosynthesis of choline phospholipids (such as phosphatidylcholine) and suggested to be altered with malignant transformation (9-11). It has been shown that inhibition of phosphocholine synthesis by novel choline kinase inhibitors exhibits antitumor activity (12,13). These data demonstrate the validity of our combined approach to produce and utilize MRS/genomic biomarker profiles to type brain tumor tissue.

Materials and methods

Tissue biopsies. Eighteen samples were analyzed: control biopsies from epileptic surgeries (10); and anaplastic ganglioglioma biopsies with grade-4 glial component changes (8). Twenty-seven separate tissue samples from 8 brain tumor patients (3 with glioblastoma multiforme, 3 with metastasis, 1 with pilocytic astrocytoma and 1 with meningioma) and 2 control patients were used to correlate HRMAS ^{1}H MRS and genomics results for the same tumor samples. The mean age for subjects was 37±14.

HRMAS ^{1}H MRS. Ex vivo HRMAS ^{1}H MRS were as described (2,4,14-18); and were performed on a Bruker Bio-Spin Avance NMR spectrometer (600.13 MHz) using a 4-mm triple resonance (^{1}H, ^{13}C, ^{2}H) HRMAS probe (Bruker). Specimens were pre-weighed and transferred to a ZrO_2 rotor tube (4-mm diameter, 50 μl), containing a permanently attached external standard (TSP or trimethylsilyl propionic-2,2,3,3-d_4 acid, M_w=172, δ=0.00 ppm), functioning as a reference both for resonance chemical shift and quantification. The HRMAS ^{1}H MRS occurred at 2˚C with 2.5 kHz MAS speed to minimize tissue degradation.

One dimensional (1-D) water suppressed, fully relaxed spectra were acquired with an optimized rotor synchronized Carr-Purcell-Meiboom-Gill (CPMG) pulse sequence [90-(τ-180-τ)$_n$-acquisition]. CPMG is preferred over simple free induction decays (FIDs), as it acts as a T2 filter that reduces the interference of very broad features in the spectrum baseline, originating from tissue water and macromolecules. Additional parameters for the CPMG sequence include inter-pulse delay (τ= 2π/ω_r = 400 μsec); n=31 (2 nτ-25 min); 256 transients; spectral width of 7.2 kHz; 8 k data points; and TR = 3 sec. For quantification purposes we measured the T2 relaxation time, by varying the CPMG evolution time (T_{CPMG} = 2nτ) [64 transients, n from 12 to 750 (~10 to 600 min)].

Further investigation of metabolite resonances were performed using an optimized version of the TOtal Correlation SpectroscopY (TOCSY) sequence (15,17,19) that employs a MLEV-17 mixing sequence for homonuclear Hartman-Hahn transfer, and water suppression. Typical TOCSY sequence parameters were spectral width 7.2 kHz; 256 steps along the first axis; 8 K complex data points along the second axis; 8 number of scans; 6 kHz rf field; mixing time = 75 min; and TR = 2 sec.

HRMAS ^{1}H MR spectral analysis. Spectra of intact specimens were analyzed using the MestRe-C NMR software package (Mestrelab Research, NMR solutions, website: www.mestrec.com). Before 1-D or 2-D Fourier transformation and phasing, all free induction decays were subjected to 1 Hz apodization. Baseline correction were performed using a low order spline function. After Lorentzian and/or Gaussian fitting, the area under the curves or the volumes of the most intense spectra resonances were calculated. Absolute or relative quantification using the external standard were performed, as described below. These resonances were identified and assigned to the corresponding metabolites. The absolute metabolic concentrations for each sample were also subjected to statistical analysis conducted by using SPSS, version 12.0 (SPSS, Chicago, IL, USA). Student's t-tests were used to compare the values between control and tumor samples. A two-tailed value of <0.05 was considered to indicate a statistically significant difference.

Quantification of brain metabolites. Precise quantification of brain metabolites from NMR measurements is complex (20). Current quantification methods can be categorized by the origin of the reference signal as either 'internal standard' or 'external standard' techniques. The 'internal standard' techniques typically use the water peak as a reference, and assume a value for the concentration of NMR-visible water; and the 'external standard' methods assume uniformity of detection sensitivity over the volume of the coil. The accuracy and precision of spectroscopic quantification, whether absolute or relative, depends on several experimental parameters, including hardware performance, such as receiver linearity, and coil characteristics; pulse sequence structure; efficiency of sequence elements, such as water suppression; and the particular method used to derive signal intensities from the spectra. Our experience indicates the 'external standard' technique provides more accurate values. We initially used 1-D spectra for quantification. All peaks that could not be well resolved using the CPMG sequence, yet appear separate in the TOCSY spectrum, were quantified from the 2-D TOCSY spectra, as described (5).

Quantification of brain metabolites from 1-D CPMG spectra. Brain metabolites were quantified with a silicone rubber, containing 10 μl 50 mM TSP, permanently attached to the sample rotor as external standard. To quantify metabolite concentration according to the external standard (STD), we measured resonance intensities for -CH3 protons of the

ibo-SPIA™ amplification process.

Three stage Ribo-SPIA amplification process used in the Ovation blotin system:	
1. First strand cDNA synthesis using a DNA/RNA primer	90 min
2. Second strand cDNA synthesis	45 min
3. SPIA™ isothermal liner amplification	75 min
Total time to prepare amplified cDNA	210 min
cDNA purification	30 min
CDNA fragmentation and biotin labeling performed in two stages:	
1. Enzymatic fragmentation	30 min
2. Biotin attachment	30 min
Total time to fragment and label amplified cDNA	60 min
Fragmented product purification, depending on sample number	30 min
Total time	330 min

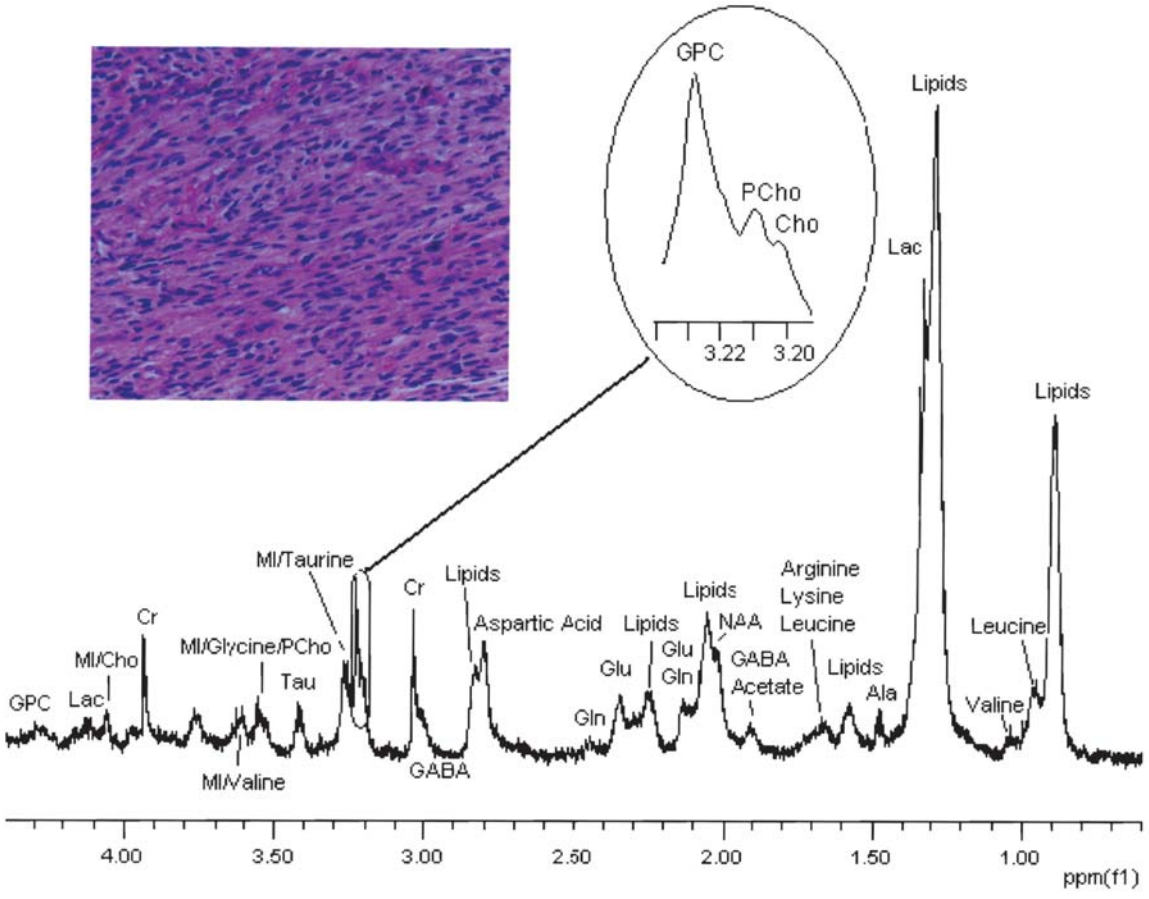

Figure 1. *Ex vivo* HRMAS ^{1}H MR spectrum of a 1.9 mg anaplastic ganglioglioma tissue biopsy. CPMG pulse sequence, total delay 2nτ of 25 min. GPC, glycerophosphocholine; PC, phosphocholine; Cho, choline; MI, myoinositol; Tau, taurine; Cr, creatine; Flu, glutamate; Gln, glutamine; Lac, lactate. Insert shows the increased cellularity of the tumor by conventional histology.

STD, as well as the difference in resonance intensities between STD and each metabolite. The absolute concentrations of the 50 most intense resonances were calculated: 1) the intensity of resonance (X), including STD, measured from the T2-filtered HRMAS ^{1}H MR spectrum were T2 corrected, using Ic(X) = Ir(X) * exp[TE/T2(X)], where Ir(X) is the measured intensity, and TE the echo time; 2) metabolite concentrations were quantified with the 'external standard' method (20), with the absolute concentration (μmol/g) of the metabolite M given by: [M] = Ic(M) * 9 * [STD]/(wt * Ic(STD) * n), where 9 is the number of protons in TSP, wt represents weight of the sample in gram and n is the number of protons

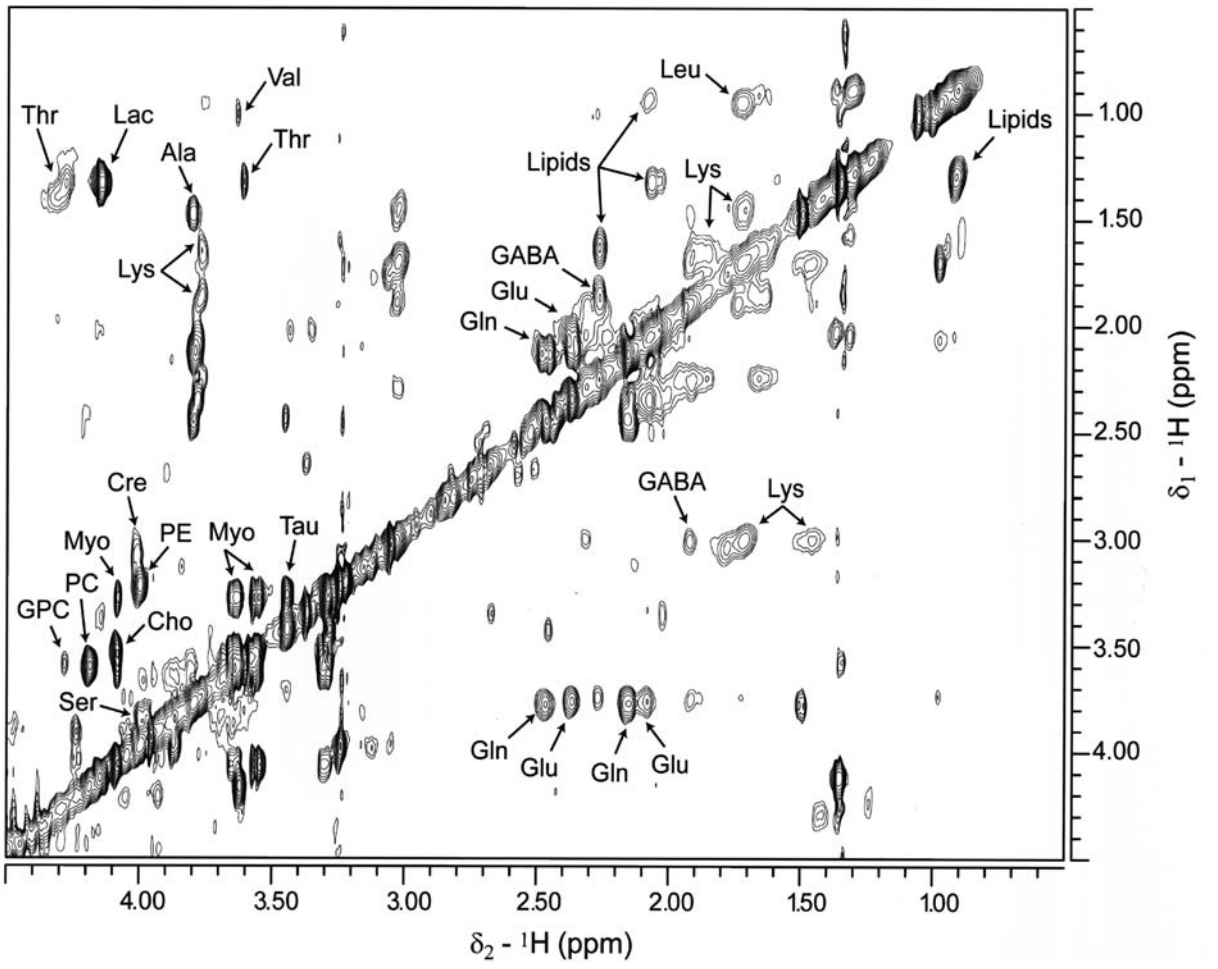

Figure 2. TOtal Correlation SpectroscopY (TOCSY) using *Ex vivo* HRMAS on a 7.3 mg anaplastic ganglioglioma tissue biopsy. HRMAS ^{1}H MR spectrum using TOCSY, with 75 min mixing time. Cho, choline; GABA, γ-aminobutyric acid; Gln, glutamine; Glu, Glutamate; GPC, glycerophosphocholine; Leu, leucine; Lys, lysine; Myo, myoinositol; PC, phosphocholine; PE, phosphoethanolamine; Ser, serine; Tau, taurine; Thr, threonine; Val, valine.

in the functional group and corresponds to the resonance of the metabolite.

Quantification of brain metabolites from 2-D TOCSY spectra. We used the glycine diagonal peak volume DPV(Gly) as reference to convert cross peak volumes of metabolites CPV(M) to peak intervals Ic(M), as described (5), using the formula: Ic(M) = (1/slope) * Ic(Gly) * CPV(M)/DPV(Gly), where slope is obtained by calibration curves that linearly correlate the TOCSY signals against fully relaxed 1-D signals. Cross peak volumes were measured in the upper half plane of the TOCSY spectrum, where they are exempt from T1 noise and partial saturation effects due to water signal suppression. The external standard method was used to further quantitate 1-D metabolite Ic(M).

Microscale genomics. The commercially available Affymetrix gene-chip U133Plus® DNA microarray (Santa Clara, CA) of the complete human genome was used to perform transcriptome profiling on each specimen for two different experimental conditions, minus or plus previous HRMAS NMR analysis. The GeneChip® microarray platform has several significant advantages over competing technologies, including coverage of the entire human genome, access to probe sequences; probe redundancy of 11 sequences per gene, which optimizes signal-to-noise ratio fidelity; ready commercial availability; standardization of the hybridization, washing, staining and scanning processes; quality control built into the manufacturing processes; available technical support; and relatively low cost per interrogated gene.

Total experimental RNA was isolated from the tumor biopsy samples. Control RNA was from normal tissue that had been removed along with the tumor tissue from a patient, or from age-matched control subjects that had undergone epilepsy surgery. RNA was isolated using the RNeasy purification kit and procedure (Qiagen), with the modification that during tissue homogenation and deproteination, 1 μg of tRNA and 10 μg linear polyacrylamide are added as carrier. This greatly improves yields to ~500 ng of total RNA per mg of tissue, which is 20-fold greater than that required for optimized RNA labeling. RNA purity was assessed from the OD 260/280 ratio, with only samples having ratios >1.9 retained for further use. In addition, RNA integrity number (RIN) was assessed on the Agilent 2100 bioanalyzer, with a sample deemed to be of good quality if it had a relatively flat and low baseline in the capillary electrophoresis elution, and its 18S and 28S peaks were from 1:1 to 1:2, as scored by the Bioanalyzer software.

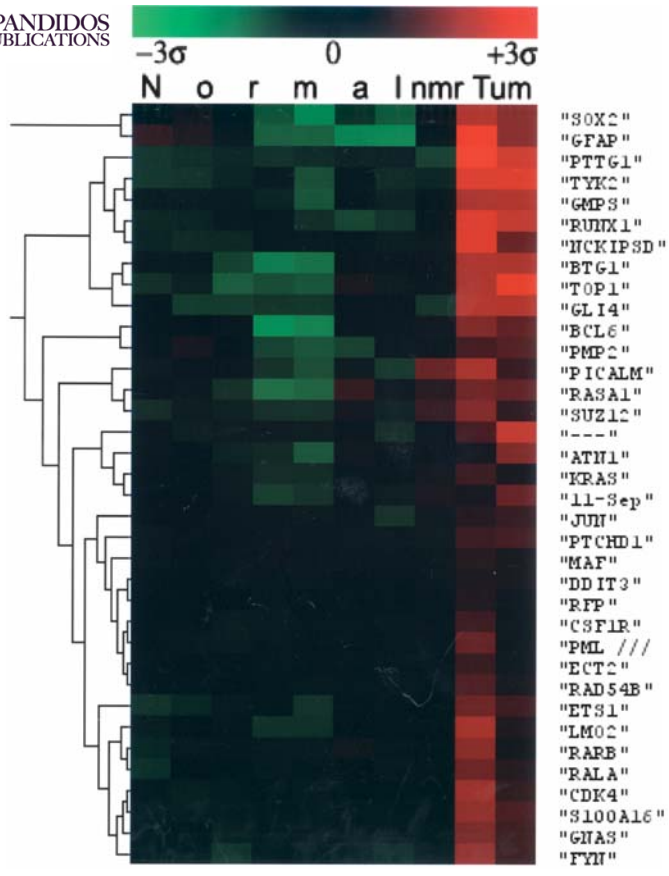

Figure 3. Effect of HRMAS on biopsy tissues. Differential expression of pro-oncogenes in control tissue after HRMAS (Normal); control without HRMAS (nmr); and tumor tissue (Tum) after HRMAS. Note that the normal and nmr patterns are similar suggesting that prior analysis of the control samples with HRMAS (nmr) does not alter gene expression.

We used the Ribonucleic acid single primer isothermal amplification (Ribo-SPIA) protocol (www.nugeninc.com) for mRNA labeling and amplification. Ribo-SPIA is a superior labeling method when <1 μg of starting RNA is used. Table I presents an overview of the Ribo-SPIA™ amplification process. Total RNA (20 ng) was used for first strand cDNA synthesis; with the entire amplification, fragmentation and labeling steps performed in a single day.

Genomic data analysis. The expression profiles from the tumor versus the control tissue biopsies were compared. Specifically, the raw expression data were analyzed for probe intensities using the the Affymetrix GeneChip expression analysis manual procedures; and the data were normalized using current R implementations of RMA algorithms (21). Following normalization, data were analyzed using methodologies that identify significant genes, classify tumor type based on expression pattern, and predict class analysis via genome wide data mining. These methods include the false discovery rate (FDR) analysis of genome-wide studies (22), significant analysis of microarrays (SAM) (23), prediction analysis for microarrays (PAM) (24,25), and tight clustering for identifying stable and tight patterns in data that can identify co-regulated gene clusters (26). This combinatorial approach reduced the chance of calling false positive genes into clusters, to improve the identification of informative genes. Results were produced in both tabular and graphical formats. For gene ontology, likelihood of over-representation of function categories in the up or downregulated gene list relative to a background of all array genes was calculated by Fisher's exact test.

Correlation of the ex vivo ^{1}H HRMAS ^{1}H MRS metabolites with the expression of relevant regulatory genes. We performed correlation analysis using least-squares fitting, to identify similarities between gene expression and MRS features by considering value patterns across the 27 analyzed samples. Genes were sorted according to the calculated least-squares error to find those that best matched the NMR metabolite data.

Results

HRMAS ^{1}H MRS. Principal metabolites were assigned by comparison to literature data (27) and Tugnoli *et al* (28) (Fig. 1). Metabolites that could not be quantified from 1-D spectra, were quantified using 2D TOCSY spectra, which exhibit excellent resolution (Fig. 2). The calibration between 2-D and 1-D spectra was obtained via linear least square fit: the average slope of the calibration curve of TOCSY measurements against 1-D fully relaxed measurements was 0.13±0.05.

Table II shows the levels of several biologically relevant metabolites are altered in anaplastic ganglioglioma tumor tissue, versus control brain tissue. Lipids, lactate, alanine, choline, phosphocholine and glutamate concentrations are significantly elevated. While taurine is also elevated, this is not statistically significant. Conversely, NAA and creatine levels are significantly reduced. While glycine is also reduced, this is not statistically significant.

Microscale genomics. Our results demonstrated that we can obtain good quality RNA from the 2 mg samples with an RNA integrity number (RIN) of 7.2±0.7 (1 = poor to 10 = excellent). Fig. 3 compares the gene expression profiles of tumor and control samples. Note that prior analysis of the control samples with HRMAS (nmr) clearly does not alter gene expression. Analysis of the microarray data using a 5% false discovery rate and a >1.4 fold change as threshold, revealed 3,614 significantly overexpressed and 929 significantly underexpressed genes in anaplastic ganglioglioma versus control tissue. Fig. 4A and B respectively identify relevant upregulated and downregulated processes.

Comparison between the group of samples that were not subjected to HRMAS NMR and the group of samples that were, has validated that the HRMAS ^{1}H MRS procedure did not degrade mRNA and that the genomic data, even with minute amounts of mRNA, were of good quality. The RNA integrity number (RIN: 1 = poor, 10 = excellent), was 7.2±0.7. Analysis of our microarray-DNA data using 5% false discovery rate and >1.4-fold change as threshold, revealed a total of 3,614 significantly overexpressed and 929 significantly underexpressed genes in tumors versus control brain.

Table III presents the differential expression of Kennedy pathway genes with emphasis on the choline kinase, which converts Cho to PCho, and the rate-regulatory gene

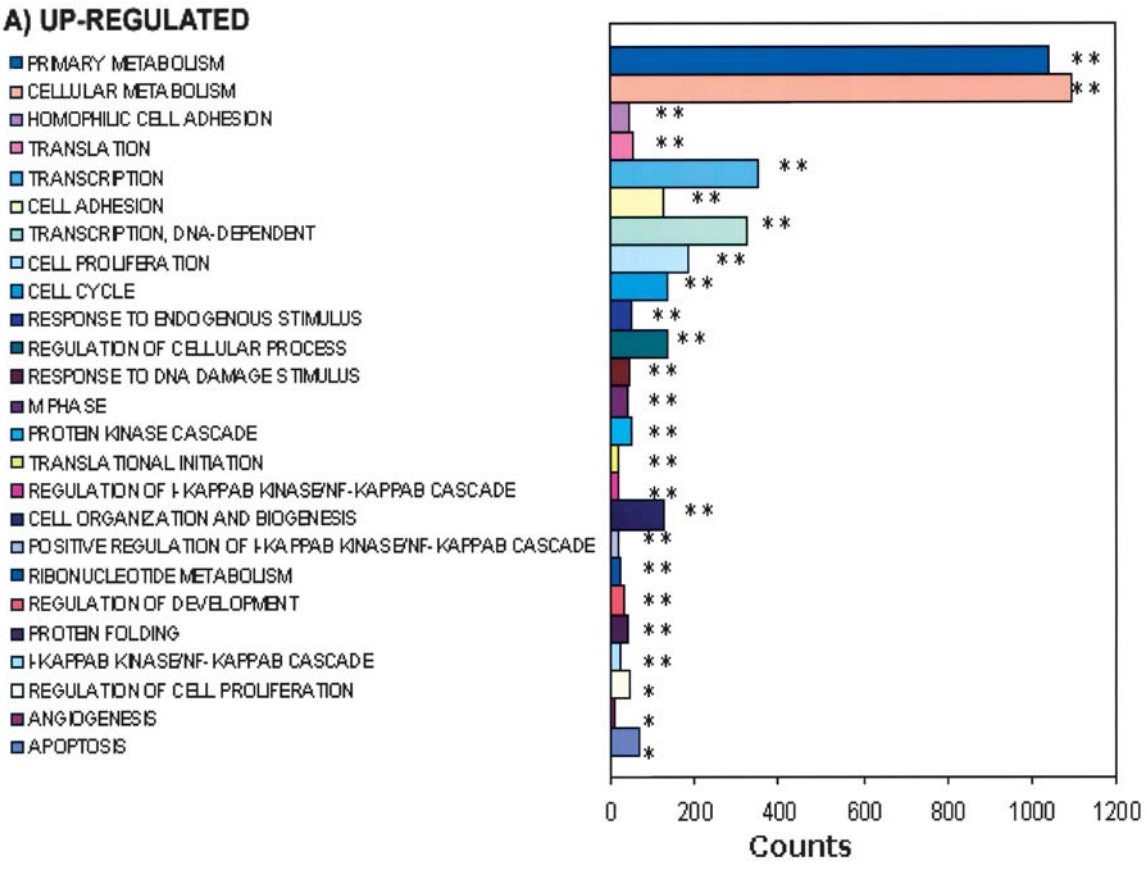

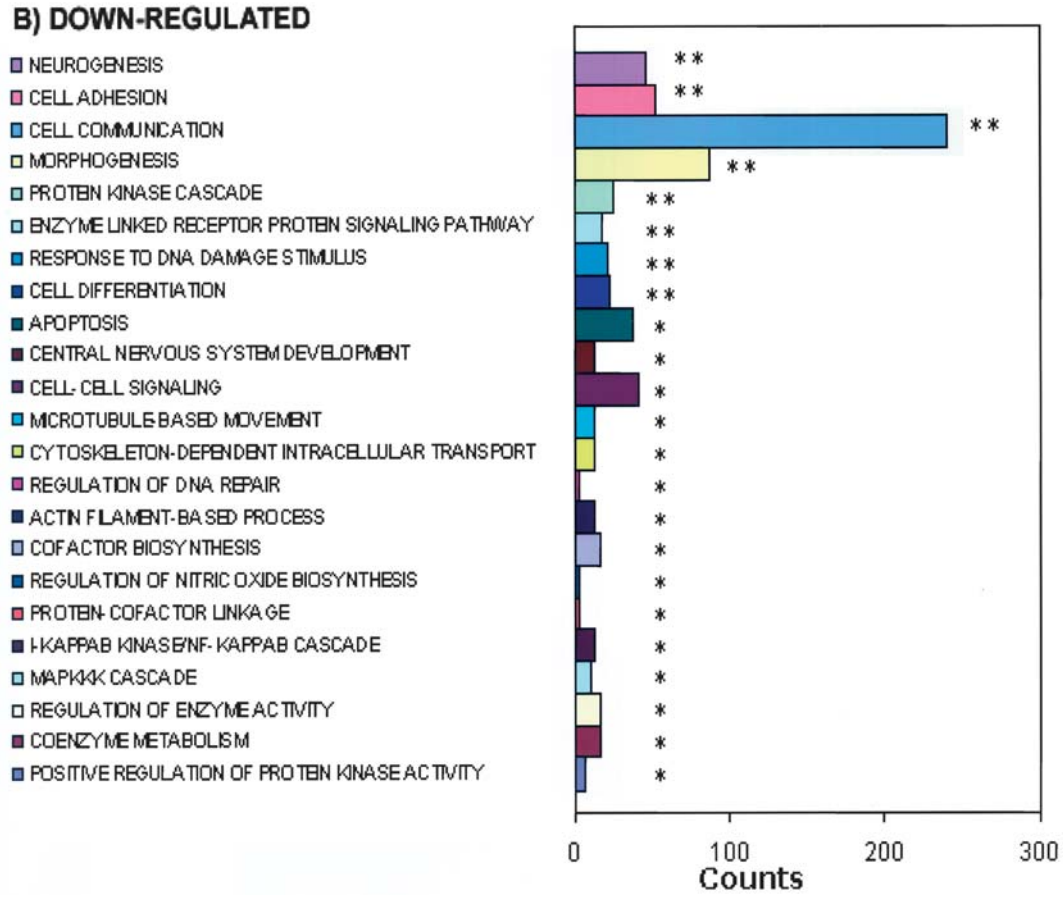

Figure 4. Functional classification of differentially upregulated or downregulated genes in anaplastic ganglioglioma brain tumor versus control tissue. Genes showing significant differential expression (cutoff of 5% false discovery rate and 1.4-fold change) were grouped for Gene Ontology-based functional classification. Color bars indicate the number of (A) upregulated and (B) downregulated genes ($^{*}P<0.05$; $^{**}P<0.01$).

Chemical shift (δ, PPM), and concentration of selected metabolites in anaplastic ganglioglioma brain tumor biopsies.

Metabolite	δ ^{1}H (ppm)	Group	Control (μmol/g)[a,c]	Brain tumor (μmol/g)[a,c]	% Δ from normal[b]	P[d]
Lipids	0.90	CH_3	4.0±0.19[a]	76.7±10.2[a]	+1817.5%	0.04
	1.29	$(CH_2)_n$	ND	200.1±32.0[a]		
	5.33	CH=CH	ND	231.9±21.8[a]		
Lactate	1.33	CH_3	40.6±0.57[a]	101.5±8.5[a]	+150.0%	0.04
Alanine	1.48	ßCH_3	4.3±0.23[a]	13.4±1.2[a]	+223.3%	0.03
NAA	2.03	CH_3	9.9±0.20[a]	5.6±0.3[a]	-43.4%	0.002
Glutamate	2.35	γCH_2	6.1±0.12[a]	47.6±5.0[a]	+680.3%	0.02
Creatine	3.04	CH_3	12.7±0.49[a]	3.3±0.3[a]	-73.9%	0.0001
	3.93	CH_2	23.1±3.7	4.7±0.5[a]	-63.5%	
Choline	3.20	$N(CH_3)_3$	0.6±0.02[a]	4.0±0.4[a]	+566.7%	0.03
			0.6±0.12[c]	3.1±0.4[c]	+416.7%	
Taurine	3.42	CH_2	6.0±0.12[a]	16.0±1.6[a]	+166.7%	0.08
			8.9±0.32[c]	16.6±2.6[c]	+86.5%	
Glycine	3.55	CH_2	22.9±0.81[a]	18.2±1.6[a]	-20.5%	0.40
PCho	3.62	CH_2	6.8±0.22[c]	23.8±1.8[c]	+250.0%	0.002
GPC	3.68	ßCH_2	ND	7.6±4.5[c]		
PE	3.99	CH_2	5.3±0.19[c]	6.1±0.9[c]	+15.1%	0.11

Values are means ± SE; [a]values from 1D CPMG measurements; [b]values are percent difference between tumor and control tissues; [c]values from 2D TOCSY measurements; [d]Student's t-test; ND, non-detectable.

CTP:phosphocholine cytidylyltransferase, which converts PCho to CDP-Cho. In addition, the expression of other genes related to membrane choline phospholipid metabolism, are listed in Table III. Note that the α and ß choline kinases are upregulated, whereas the choline transporters (CHT1, gene symbol SLC5A7; OCT1, gene symbol SLC22A1; OCT2, gene symbol SLC22A2; CTL3, gene symbol SLC22A13; and CTL4, gene symbol SLC22A14) are either unchanged, or down-regulated (CTL1, gene symbol SLC44A1). Phosphocholine cytidylyltransferase α gene PCYT1A is slightly upregulated, whereas the ß gene PCYT1B is hardly changed. The greatest change is in phospholipase C, which is upregulated and likely contributes to the elevated PCho levels.

Correlation analysis. Our correlation analysis algorithm produced easily identifiable one-to-one correlations in 27 biopsies, and revealed significant correlations between MRS and gene expression values ($r>0.7$, $P<0.001$) (Fig. 5). The correlation between the MRS and genomics data was calculated using the least-squares fit. The scaled gene expression values of the first 50 best-matching genes (having the lowest Chi-square value) are plotted together with the MRS data, for each of the biopsies.

Discussion

The present study is the first to demonstrate the feasibility and validity of combining MRS and transcriptome analyses to produce combinatorial biochemical and molecular biomarker profiles from microscale tissue biopsy specimens. We suggest that our combinatorial approach is superior to combining HRMAS ^{1}H MRS of intact brain tumor biopsies with histopathology, as proposed previously by Cheng and colleagues (2). Although this suggestion is not based on the data presented herein, prior work has shown that both MRS and expression microarray data predict survival better than does standard histopathology (7,29). As such, our MRS/genomics approach should improve the clinical diagnosis and treatment of CNS tumors. In addition, this approach should be applicable to other microscale samples, such as non-CNS tissue biopsies, and stem cell populations.

We emphasize here, MRS data indicated that elevated phosphocholine (PCho) in anaplastic ganglioglioma (Table II) was primarily attributable to overexpression of choline kinase and phospholipase C detected in the microarray analysis (Table III). In general, as shown in Table II, neoplasia affects the levels of brain metabolites the most important of which

Table III. Differential expression of choline metabolism genes in anaplastic ganglioglioma brain tumor biopsies.

GenBank Accession No.	Name of gene	Gene symbol	Fold change tumor/control[a]
NM_016341	Phospholipase C, ε1	PLCE1	5.56
NM_002660	Phospholipase C, γ1	PLCG1	2.34
NM_005198	Choline kinase ß	CHKB	1.71
NM_015192	Phospholipase C, ß1 (phosphoinositide-specific)	PLCB1	1.66
NM_001277	Choline kinase α	CHKA	1.26
NM_178034	Phospholipase A2, group IVD (cytosolic)	PLA2G4D	1.23
NM_005017	Phosphate cytidylyltransferase 1, choline, α	PCYT1A	1.16
NM_021213	Phosphatidylcholine transfer protein	PCTP	1.12
NM_004845	Phosphate cytidylyltransferase 1, choline, ß	PCYT1B	0.94
NM_021815	Solute carrier family 5 (choline transporter), member 7	SLC5A7	0.89
NM_002661	Phospholipase C, γ2 (phosphatidylinositol-specific)	PLCG2	0.86
NM_002662	Phospholipase D1, phophatidylcholine-specific	PLD1	0.86
NM_004803	Solute carrier family 22 (organic cation transporter), member 14	SLC22A14	0.85
NM_004256	Solute carrier family 22 (organic cation transporter), member 13	SLC22A13	0.83
NM_001007794	Choline/ethanolamine phosphotransferase 1	CEPT1	0.82
NM_003058	Solute carrier family 22 (organic cation transporter), member 2	SLC22A2	0.77
NM_024420	Phospholipase A2, group IVA (cytosolic, calcium-dependent)	PLA2G4A	0.76
NM_015900	Phospholipase A1 member A	PLA1A	0.72
NM_003057	Solute carrier family 22 (organic cation transporter), member 1	SLC22A1	0.71
NM_020244	Choline phosphotransferase 1	CHPT1	0.61
NM_022109	Solute carrier family 44, member 1	SLC44A1	0.36

[a]Values are the relative expression intensity of the tumor versus the control tissue. Values >1 denote upregulated genes; values <1 denote downregulated genes.

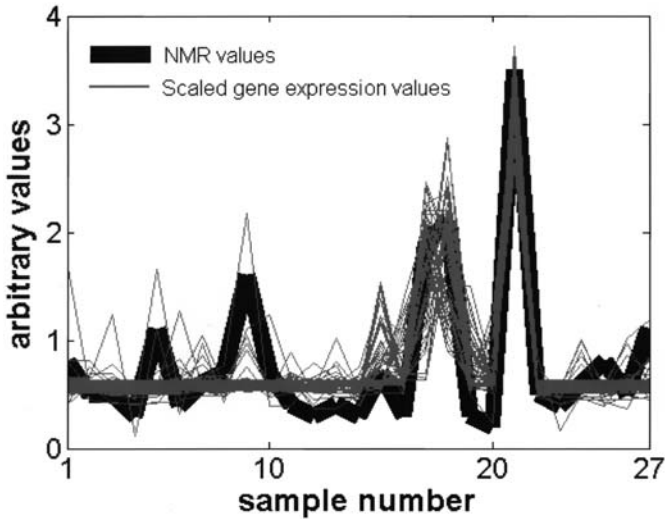

Figure 5. Correlation analysis demonstrates strongly identifiable one-to-one correlations in 27 biopsies and reveals significant correlations between MRS and gene expression values ($r>0.7$, $P<0.001$). Black line, MRS quantitation data. Grey line, scaled expression values of the first fifty genes having the highest correlation with the MRS data (least-squares fit). X-axis; the respective sample numbers (1-27).

can qualify as sensitive and accurate biomarkers not only of diagnostic value but also of prognosis and include lipids, lactate, alanine, NAA, glutamate, creatine, choline-containing compounds, such as phosphocholine, glycerophosphocholine and free choline, phosphoethanolamine, taurine and perhaps glycine and this is in accordance with previous published reports (1,3,16,28-35). Also, our quantitative MRS results herein are in agreement with previous published reports (27).

In addition, our differential gene expression results show that anaplastic ganglioglioma tumor tissue, consistent with its non-neuronal derivation, has altered expression for glial lineage genes, i.e., SOX2, GFAP, PMP2, S100A18; and cell differentiation genes, i.e., TYK2 (Fig. 3). Furthermore, PTCHD1, a transcriptional target of the Sonic Hedgehog pathway (SHH) is differentially expressed, as well as the downstream SHH targets, GLI4 and NCKIPSD (Fig. 3). These data suggest SHH dysregulation may play a role in anaplastic ganglioglioma pathogenesis which adds to the almost non-existent knowledge regarding the biological behavior of this tumor.

A principal finding of our experiments herein is that the levels of specific MRS-derived metabolites (Table II) are altered in concert with the expression of genes (Table III) that mediate the Kennedy pathway for *de novo* synthesis of phosphatidylcholine (PtCho), which is essential for the production of membrane PtCho, a key component of nucleated cells. This pathway, discovered in the 1950s by Eugene Kennedy and presented in Fig. 6, has been extensively studied; and its activation and regulation depend on Cho transporters and choline kinase upregulation, to produce Cho-containing

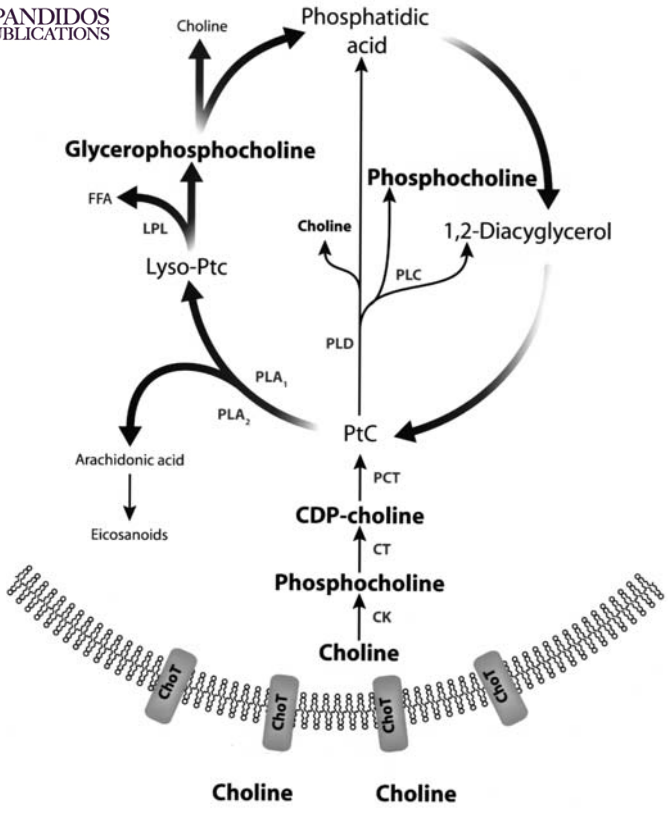

Figure 6. Fate of choline-containing compounds in the Phosphatidylcholine (PtC) cycle. Phosphorylation of choline to phosphocholine (PCho) by choline kinase (CK) is the first step following choline transport across the plasma cell membrane by various choline transporters (ChoT), with transport the rate-limiting step in Pcho synthesis. PCho is then converted to PtC via phosphocholine cytidyltransferase (CT) and phosphocholine transferase (PCT), intermediates of the rate-limiting enzyme CTP. PtC hydrolysis is effected by the three PtC-specific enzymes, phospholipase C (PLC), phospholipase D (PLD), and phospholipase A1 and A2 (PLA1 and PLA2). FFA, free fatty acid. Compounds in black bolded font correspond to MRS-detected compounds, grey bolded font corresponds to enzymes whose expression is assessed by genomics.

compounds, and thus more substrate. Our findings are consistent with choline kinase upregulation which activates the Kennedy pathway, which produces Cho-containing compounds, and thus more substrate. Cho transporters are downregulated due to intracellular substrate accumulation. The genomic data support and cross validate the Table II MRS data and are in agreement with published data in breast cancer (11); but differ from others reporting enhanced choline transport and augmented synthesis of phosphocholine as dominant pathways responsible for the elevated presence of choline metabolites in cancerous breast tumors (36). However, our data show corresponding changes in Cho, PCho, GPC and PE, and suggest rapid phospholipid turnover, which coincides with upregulated cell proliferation (Fig. 4A). Thus, Tables II and III cross validate the MRS and genomic data.

In addition, these data support the hypothesis that products of membrane choline phospholipid metabolism, such as PCho, diacylglycerol, and arachidonic acid metabolites, function as second messengers essential for the mitogenic activity of growth factors and pathways, including the *ras-raf-1-MAPK* and protein kinase C pathways (10). Furthermore, they accord with the observations that Cho metabolism and choline-derived metabolites are altered in human breast malignancies (10,37,38). As such, our combinatorial approach could identify biologically significant biomarkers that can be used as surrogate *in vivo* markers to monitor the efficiency of anti-cancer therapies that specifically aim to inhibit membrane phospholipid metabolism.

Since the diagnostic utility of biomarkers for tissue fingerprinting lies in their biological relevance, highly informative biomarker profiles are difficult to establish, as neuropathology for tumor typing is limited. According to a previous report, expression microarray data suggest that molecular profiles of biomarkers classify malignant gliomas and predict survival better than does standard histopathology (7). Recently, it was shown that brain proton MRS imaging biomarkers predict survival of children with CNS tumors better than does standard histopathology (29). On the other hand, the small sample size of tissue biopsies poses technical challenges for producing accurate transcriptome data.

Since CNS tumor biopsies are often highly size restricted, and this limitation can make their analysis technically challenging, in particular for the production of accurate transcriptome data, our combinatorial microscale approach is significant to identify biomarker profiles that can facilitate typing of tumor biopsies of only 2 mg in size. While we focus here on brain tumors, microscale MRS and genomics are equally relevant to other medically important tissues that are size limited, such as other clinical biopsies, and stem cell populations. As we have shown herein, we can produce excellent quality data and the data from two different sources, MRS metabolomics and genomics, correlate well (Fig. 5).

We believe that the results from this study provide insights into the biology of anaplastic ganglioglioma, and further demonstrate the biological relevance of MRS-based biomarkers as potential surrogate *in vivo* biomarkers to non-invasively diagnose inoperable cancers and monitor their treatment.

Acknowledgements

The study was supported in part by a grant of the American Cancer Society Grant RPG-98-056-01-CCE to A. Aria Tzika and by a Center grant of the National Institutes of Health to the Stanford Genome Technology Center. The authors thank the Departments of Surgery and Radiology at Massachusetts General Hospital, as well as Neurosurgery and Pathology at Children's Hospital Boston for supporting this study. We also thank Dr Scott Stachel for editorial assistance.

References

1. Astrakas LG, Zurakowski D, Tzika AA, *et al*: Noninvasive magnetic resonance spectroscopic imaging biomarkers to predict the clinical grade of pediatric brain tumors. Clin Cancer Res 10: 8220-8228, 2004.
2. Cheng LL, Ma MJ, Becerra L, *et al*: Quantitative neuropathology by high resolution magic angle spinning proton magnetic resonance spectroscopy. Proc Natl Acad Sci USA 94: 6408-6413, 1997.
3. Cheng LL, Anthony DC, Comite AR, Black PM, Tzika AA and Gonzalez RG: Quantification of microheterogeneity in glioblastoma multiforme with *ex vivo* high-resolution magic-angle spinning (HRMAS) proton magetic resonance spectroscopy. Neuro-Oncology 2: 87-95, 2000.

4. Tzika AA, Cheng LL, Goumnerova L, *et al*: Biochemical characterization of pediatric brain tumors by using *in vivo* and *ex vivo* magnetic resonance spectroscopy. J Neurosurg 96: 1023-1031, 2002.
5. Morvan D, Demidem A, Papon J, De Latour M and Madelmont JC: Melanoma tumors acquire a new phospholipid metabolism phenotype under cystemustine as revealed by high-resolution magic angle spinning proton nuclear magnetic resonance spectroscopy of intact tumor samples. Cancer Res 62: 1890-1897, 2002.
6. Pomeroy SL, Tamayo P, Gaasenbeek M, *et al*: Prediction of central nervous system embryonal tumour outcome based on gene expression. Nature 415: 436-442, 2002.
7. Nutt CL, Mani DR, Betensky RA, *et al*: Gene expression-based classification of malignant gliomas correlates better with survival than histological classification. Cancer Res 63: 1602-1607, 2003.
8. Hakim R, Loeffler JS, Anthony DC and Black PM: Gangliogliomas in adults. Cancer 79: 127-131, 1997.
9. Podo F: Tumour phospholipid metabolism. NMR Biomed 12: 413-439, 1999.
10. Aboagye EO and Bhujwalla ZM: Malignant transformation alters membrane choline phospholipid metabolism of human mammary epithelial cells. Cancer Res 59: 80-84, 1999.
11. Glunde K, Jie C and Bhujwalla ZM: Molecular causes of the aberrant choline phospholipid metabolism in breast cancer. Cancer Res 64: 4270-4276, 2004.
12. Hernandez-Alcoceba R, Saniger L, Campos J, *et al*: Choline kinase inhibitors as a novel approach for antiproliferative drug design. Oncogene 15: 2289-2301, 1997.
13. Hernandez-Alcoceba R, Fernandez F and Lacal JC: *In vivo* antitumor activity of choline kinase inhibitors: a novel target for anticancer drug discovery. Cancer Res 59: 3112-3118, 1999.
14. Sivaraja M, Turner C, Souza K and Singer S: *Ex vivo* two-dimensional proton nuclear magnetic resonance spectroscopy of smooth muscle tumors: advantages of total correlated spectroscopy over homonuclear J-correlated spectroscopy. Cancer Res 54: 6037-6040, 1994.
15. Middleton DA, Bradley DP, Connor SC, Mullins PG and Reid DG: The effect of sample freezing on proton magic-angle spinning NMR spectra of biological tissue. Magn Reson Med 40: 166-169, 1998.
16. Cheng LL, Chang IW, Louis DN and Gonzalez RG: Correlation of high-resolution magic angle spinning proton magnetic resonance spectroscopy with histopathology of intact human brain tumor specimens. Cancer Res 58: 1825-1832, 1998.
17. Millis K, Weybright P, Campbell N, *et al*: Classification of human liposarcoma and lipoma using *ex vivo* proton NMR spectroscopy. Magn Reson Med 41: 257-267, 1999.
18. Tate AR, Foxall PJ, Holmes E, *et al*: Distinction between normal and renal cell carcinoma kidney cortical biopsy samples using pattern recognition of (1)H magic angle spinning (MAS) NMR spectra. NMR Biomed 13: 64-71, 2000.
19. Weybright P, Millis K, Campbell N, Cory DG and Singer S: Gradient, high-resolution, magic angle spinning ^{1}H nuclear magnetic resonance spectroscopy of intact cells. Magn Reson Med 39: 337-345, 1998.
20. Keevil SF, Barbiroli B, Brooks JC, *et al*: Absolute metabolite quantification by *in vivo* NMR spectroscopy: II. A multicentre trial of protocols for *in vivo* localised proton studies of human brain. Magn Reson Imaging 16: 1093-1106, 1998.
21. Irizarry RA, Hobbs B, Collin F, *et al*: Exploration, normalization, and summaries of high density oligonucleotide array probe level data. Biostatistics 4: 249-264, 2003.
22. Storey JD and Tibshirani R: Statistical significance for genomewide studies. Proc Natl Acad Sci USA 100: 9440-9445, 2003.
23. Tusher VG, Tibshirani R and Chu G: Significance analysis of microarrays applied to the ionizing radiation response. Proc Natl Acad Sci USA 98: 5116-5121, 2001.
24. Tibshirani R, Hastie T, Narasimhan B and Chu G: Diagnosis of multiple cancer types by shrunken centroids of gene expression. Proc Natl Acad Sci USA 99: 6567-6572, 2002.
25. Bair E and Tibshirani R: Semi-supervised methods to predict patient survival from gene expression data. PLoS Biol 2: E108, 2004.
26. Tseng GC and Wong WH: Tight clustering: a resampling-based approach for identifying stable and tight patterns in data. Biometrics 61: 10-16, 2005.
27. Govindaraju V, Young K and Maudsley AA: Proton NMR chemical shifts and coupling constants for brain metabolites. NMR Biomed 13: 129-153, 2000.
28. Tugnoli V, Schenetti L, Mucci A, *et al*: A comparison between *in vivo* and *ex vivo* HR-MAS ^{1}H MR spectra of a pediatric posterior fossa lesion. Int J Mol Med 16: 301-307, 2005.
29. Marcus KJ, Astrakas LG, Zurakowski D, *et al*: Predicting survival of children with CNS tumors using proton magnetic resonance spectroscopic imaging biomarkers. Int J Oncol 30: 651-657, 2007.
30. Kinoshita Y and Yokota A: Absolute concentrations of metabolites in human brain tumors using *in vitro* proton magnetic resonance spectroscopy. NMR Biomed 10: 2-12, 1997.
31. Tugnoli V, Tosi MR, Tinti A, Trinchero A, Bottura G and Fini G: Characterization of lipids from human brain tissues by multi-nuclear magnetic resonance spectroscopy. Biopolymers 62: 297-306, 2001.
32. Tzika AA, Zarifi MK, Goumnerova L, *et al*: Neuroimaging in pediatric brain tumors: Gd-DTPA-enhanced, hemodynamic, and diffusion MR imaging compared with MR spectroscopic imaging. Am J Neuroradiol 23: 322-333, 2002.
33. Tzika AA, Astrakas LG, Zarifi MK, *et al*: Spectroscopic and perfusion magnetic resonance imaging predictors of progression in pediatric brain tumors. Cancer 100: 1246-1256, 2004.
34. Griffin JL and Shockcor JP: Metabolic profiles of cancer cells. Nat Rev Cancer 4: 551-561, 2004.
35. Griffin JL and Kauppinen RA: A metabolomics perspective of human brain tumours. FEBS Lett 274: 1132-1139, 2007.
36. Katz-Brull R, Seger D, Rivenson-Segal D, Rushkin E and Degani H: Metabolic markers of breast cancer: enhanced choline metabolism and reduced choline-ether-phospholipid synthesis. Cancer Res 62: 1966-1970, 2002.
37. Singer S, Souza K and Thilly WG: Pyruvate utilization, phosphocholine and adenosine triphosphate (ATP) are markers of human breast tumor progression: a 31P- and 13C-nuclear magnetic resonance (NMR) spectroscopy study. Cancer Res 55: 5140-5145, 1995.
38. Ting YL, Sherr D and Degani H: Variations in energy and phospholipid metabolism in normal and cancer human mammary epithelial cells. Anticancer Res 16: 1381-1388, 1996.